

TIME COURSE AND DISTRIBUTION OF TUNGSTEN-LADEN MACROPHAGES IN THE HILAR LYMPH NODES OF THE DOG LUNG AFTER EXPERIMENTAL INSTILLATION OF CALCIUM TUNGSTATE INTO THE LEFT APICAL BRONCHUS

N.R. Grande, C. Moreira de Sá, A.P. Águas, E. Carvalho, M. Soares

Department of Anatomy, Abel Salazar Institute for the Biomedical Sciences (NRG,APA,EC,MS), Metallurgic and Material Sciences Center of the Engineering Faculty (CMdS) and Center for Experimental Cytology (APA), University of Porto, Porto, Portugal

ABSTRACT

We sprayed a tungsten powder (CaWO₄) into the airway of a single lobe (left apical) of the dog lung in order to study: (a) the kinetics of particle translocation from the bronchoalveolar lining to hilar lymph nodes, and (b) the sorting in lung lymph nodes of inhaled microcrystals. We found that the transport of the tungsten particles to the regional lymph node takes at least 24 hours and reaches its peak at day 7. In situ detection of tungsten by elemental particle analysis of lymph node sections by scanning electron microscopy allowed precise mapping of the marker in the node; the method was complemented by light microscopy and thin-section electron microscopy of the same nodes. Virtually all of the lymph node tungsten was located inside macrophages. The first tungsten-positive macrophages seen in the regional lymph nodes (day 1 to day 3) were restricted to the subcapsular space. This was followed by massive filling of the same sinus and of the narrow interfollicular areas by the particle-laden macrophages (day 3 to day 7). The even distribution of the tungsten-bearing phagocytes found in these anatomical regions of the node indicated that the subcapsular area in the dog was a continuous domain rather than the segmented region observed in nodes of

common laboratory animals such as the rat. By day 7 after tungsten instillation, a moderate number of tungsten-positive macrophages was also detected in the paracortical region of the node. Finally, the presence of tungsten-bearing macrophages was extended to the outer lymph node medulla (day 7 to day 14); here, the macrophages were located in association with cords of plasmacytes and showed interdigitations with these lymphocytes. Only minimal amounts of tungsten were detected inside lymphoid follicles in association with dendritic cells. Some of the tungsten initially deposited in the airway of the apical left lung lobe was detected in contralateral hilar lymph nodes.

We conclude that: (i) particle translocation from the alveolus to regional lymph nodes is a slow process that is mediated by pulmonary macrophages, in agreement with the findings of Harmsen et al (Science 230:1277, 1985); (ii) in the lymph node, particle-bearing macrophages are sorted through narrow interfollicular sinuses into the outer medulla where they interact extensively with plasma cells; (iii) the migrating macrophages cannot penetrate the follicular domains of the node; minute quantities of exogenous particles may, nevertheless, be transferred from macrophages to follicular dendritic cells; and (iv) contralateral drainage may be a feature of the lymphatic system in the lung.

The lymph node is a component of the peripheral immune system of mammals that participates in the defense against particles and microorganisms that penetrate the skin or the body's mucosal linings. These foreign elements are usually transported to regional lymph nodes where an immune response may follow their presentation to lymphoid cells (1). The lymph node is organized into anatomical domains that show immunophysiological individuality as exemplified by the well-established B and T-cell zones within the node (2-4). Consequently, the definition of the sorting by the lymph node tissue of exogenous components has been the subject of a number of studies and of some controversy (see, for instance, refs. 5-8). Current views on topography of the lymph node domains are based primarily on physiologic data derived from examination of lymph nodes after subcutaneous injection of particulate tracers. In these experimental models, a significant complement of the injected particles reaches the draining lymph node as free, extracellular elements carried in by the lymph flow. In the pulmonary system, in contrast, the elegant studies by Harmsen and co-workers (9,10) revealed that airway deposited particles are translocated intracellularly by phagocytes that carry them from the alveolus to the hilar lymph nodes. Furthermore, they demonstrated that the macrophage that engulfs the particles at the bronchoalveolar lining is the same cell that reaches the regional node (9). This peculiarity of the sorting of exogenous particles in the lung led us to study the anatomy of hilar lymph nodes after the experimental instillation of microparticles in the canine airway.

We report here on the time course and topography of particle-laden macrophages within pulmonary lymph nodes of the dog following the experimental instillation of calcium tungstate in the airway of the left upper lung lobe. Samples of the hilar lymph nodes were studied as follows: cell suspensions from lymph nodes were evaluated using light microscopy for the presence of granulocytes and tungsten-bearing macrophages; sections of

lymph node were examined using light microscopy, transmission electron microscopy, and elemental particle analysis coupled to scanning electron microscopy for the localization of tungsten deposits. The integration of the results obtained with the different methods provided a comprehensive view of the movement of inflammatory macrophages into and within hilar lymph nodes of the lung.

MATERIALS AND METHODS

Animals

Twelve male and female adult mongrel dogs were used. The dogs were housed individually in kennels, fed standard commercial dog food, and had unrestrained access to water. Food and water were withheld overnight before anesthesia.

Experimental Protocol

Dogs were anesthetized by intravenous injection of sodium pentobarbital (40mg/kg of weight) and the left bronchus was surgically exposed. The airway of the apical left lobe of the lung was sprayed with 5g of calcium tungstate (CaWO_4 ; Aldrich Chemical Company, Inc., Milwaukee, WI, USA) upon the cannulation of its lobar bronchus. We chose CaWO_4 as the particle marker because of several advantageous features: 1) It is a water-insoluble, non-antigenic dry powder of an exceedingly rare component of the normal breathing atmosphere; 2) it is made up of tetragonal crystals that are small enough (less than 10μ in length) to reach the alveoli; 3) it is readily identifiable by light microscopy because of its autofluorescence and refringency (expressed by a yellow-green color); 4) it can be specifically identified in scanning electron microscopic preparations upon elemental detection of tungsten; 5) as it is a heavy metal salt, it leads to electron dense inclusions in thin section electron microscopic preparations.

The dogs were divided into four groups of two dogs each that were sacri-

ficed 1, 3, 7, and 14 days after the CaWO_4 instillation in the left upper lung lobe. Two additional groups of two dogs each were used to control the cytological scoring of inflammatory granulocytes and CaWO_4 -positive cells: the dogs of the first group were left untreated; the dogs from the latter group were sham-operated, no calcium tungstate was instilled, and they were sacrificed 14 days after surgery. The study was designed up to 14 days after lung instillation of CaWO_4 because this time period is when the local immune response reaches its peak in the dog (11,12). All dogs were sacrificed by intravenous injection of a lethal dose of sodium pentobarbital followed by exsanguination. Samples of the following hilar lymph nodes were collected: left and right, upper and lower lymph nodes, and large medial lymph node (located just underneath the tracheal bifurcation). A sample of lung tissue was also collected and used to check that a successful instillation of CaWO_4 in the left upper lobe had been achieved. The lymph node specimens were processed for (1) light microscopy; (2) thin-section electron microscopy; (3) scanning electron microscopy.

Light microscopy

Cell suspensions of lymph node tissue were obtained after the incubation of finely minced samples in 0.5% collagenase, 10mM EDTA, 0.34M sucrose in phosphate buffered saline (PBS), pH 7.4, at 37°C for 1 hour, and used to obtain cytocentrifuge slides that were stained with Wright's stain. The identification of CaWO_4 -positive macrophages was determined based on the peculiar refringence (yellow-green color) and on the autofluorescence of CaWO_4 inclusions. The cytocentrifuge preparations were used to determine the following quantitative parameters: (i) percent of granulocytes present among the population of lymph node phagocytes (macrophages, monocytes and granulocytes); (ii) percent of lymph node macrophages that contain tungsten inclusions. At least 300 cells were counted in each slide. Semithin (1-

2 μ) sections of Epon embedded samples (see next paragraph) were also studied by light microscopy to determine the positioning of tungsten-laden macrophages in the lymph node tissue and, thus, confirm the results obtained by elemental analysis scanning electron microscopy.

Transmission electron microscopy

The lymph node samples were fixed for 24 hours at room temperature in an aldehyde mixture made up of 4% formaldehyde, 1.25% glutaraldehyde, and 10mM CaCl_2 in 0.05M cacodylate buffer (13). The specimens were washed in buffer, and postfixed in 1% osmium tetroxide and in 0.5% uranyl acetate (14), dehydrated through a series of graded ethanol steps, and embedded in Epon. All resin-embedded specimens were sectioned in a LKB ultramicrotome and the thin sections stained with uranyl acetate and lead citrate. The preparations were viewed in a Siemens Elmiskop 1A or in a JEOL 100C electron microscope.

Scanning electron microscopy

Aldehyde fixed and washed samples (see previous paragraph) were dehydrated in ethanols and critical-point-dried in a Balzers apparatus using carbon dioxide as the transitional fluid. The preparations were coated by Au/Pt under vacuum and examined in a JEOL ISM-35C scanning electron microscope. The electron micrographs were derived from secondary or retrodiffused electrons, the latter mode being used to detect tungsten *in situ* by elemental particle analysis of the tissue preparations.

RESULTS

Quantification of granulocytes and of tungsten-laden macrophages in the hilar lymph nodes

Cytocentrifuge preparations of cell suspension were used to determine the percentage of inflammatory cells present in the hilar lymph nodes after CaWO_4

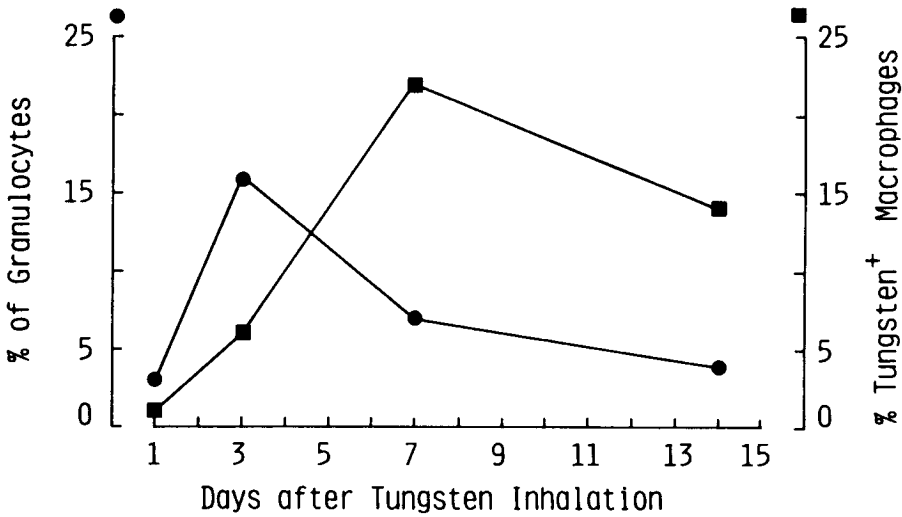


Fig. 1. Kinetics of inflammatory cells in the left upper hilar lymph node after tungsten deposition in the airway of the left upper lobe of the dog lung. ● percent of granulocytes in the total population of lymph node phagocytes; ■ macrophages containing tungsten inclusions (percent in total population of macrophages).

inhalation (Fig. 1). Few granulocytes were detected in the regional lymph node of the two dogs studied 24 hours after instillation of CaWO_4 into the left apical lobe of the lung. In fact, the percentage of granulocytes in the total number of lymph node phagocytes observed at 24 hours (3%) was similar to the percentage (2%) of granulocytes present in control dogs. The lymph node granulocytes reached their peak at day 3 (16%), and decreased thereafter (7% at day 7; and 4% at day 14). Of the granulocytes observed in the lymph node, few contained tungsten-positive inclusions: at day 3, for instance, less than 10% of the granulocytes observed presented tungsten inclusions. At day 3, a few granulocytes (4%) were seen inside large macrophages; these macrophages were tungsten positive.

Tungsten was absent or very scarce in the regional lymph node 24 hours after tungsten spraying of the left apical bronchus. The percentage of tungsten-positive macrophages detected in the regional lymph node increased from day 3 (6%) to day 7 (22%), and was found to be lower at day 14 (14%; Fig. 1). It should be

taken into account, however, that at day 14 the tungsten inclusions appeared to occupy a larger volume of the cytoplasm in each tungsten-positive macrophage than at day 7. After day 7, tungsten not only was detected in the regional lymph node but also in the medial tracheobronchial lymph node and in the right tracheobronchial node (Table 1). Tungsten inclusions were seldom found in the lower hilar lymph nodes.

Table 1
Comparison of CaWO_4 -Positive Macrophages Among Three Differently Located Tracheobronchial Lymph Nodes (LN) 3, 7, and 14 Days After CaWO_4 Deposition in the Airway of the Left Upper Lobe of the Canine Lung

Day	Left LN (%)		Medial LN (%)		Right LN (%)	
3	5-10	5-10	<5	0	0	0
7	>15	>15	5-10	5-10	0	0
14	10-15	10-15	10-15	10-15	<5	<5

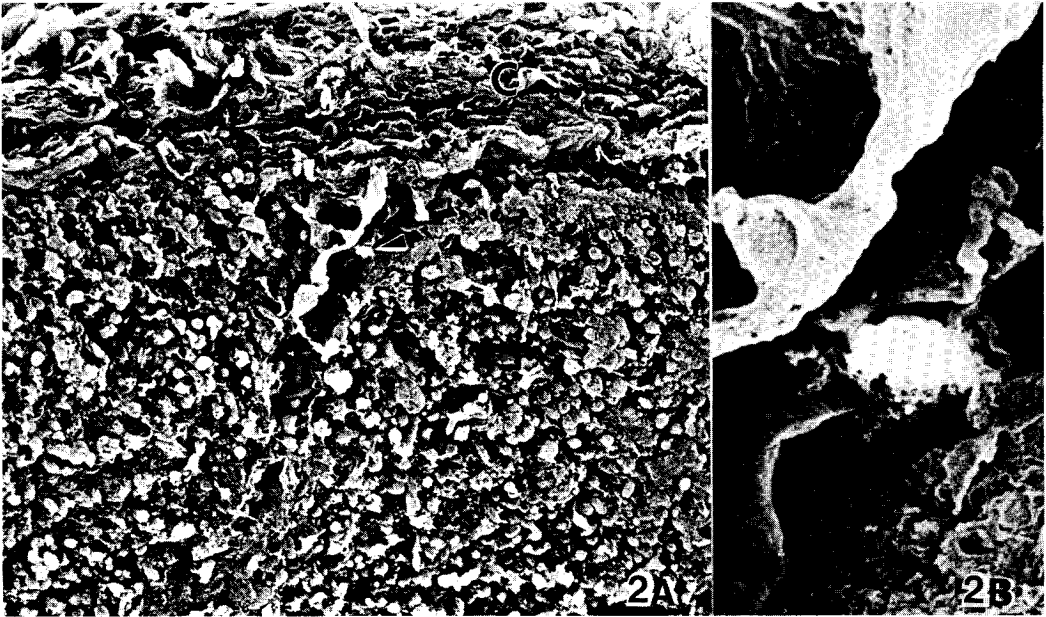


Fig. 2A and B. Scanning electron micrographs of a subcapsular region of a lower left lymph node 7 days after tungsten instillation in the airway of the upper left lobe of the lung. The elemental analysis mode picks up a single tungsten-positive cell (arrowhead in 2A; white spot in 2B) in a large tissue area. C = capsule. 2A—low magnification (x1450); 2B—high magnification of the area with the tungsten-positive cell (x8400).

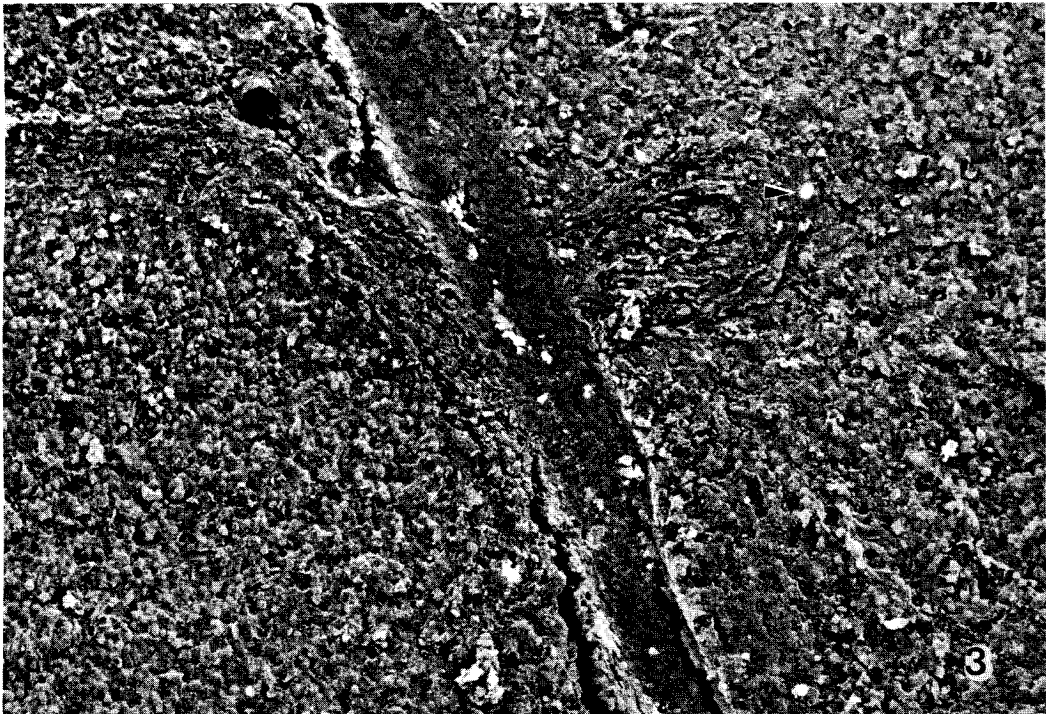


Fig. 3. Scanning electron micrograph of the cortex of regional lymph node 3 days after tungsten instillation in the airway. The few large tungsten inclusions (white spots) are found in the interfollicular sinuses. A few tungsten-positive cells reach the interface between the sinuses and the lymphoid follicles (arrowhead). x1350.

Permission granted for single print for individual use.

Reproduction not permitted without permission of Journal LYMPHOLOGY.

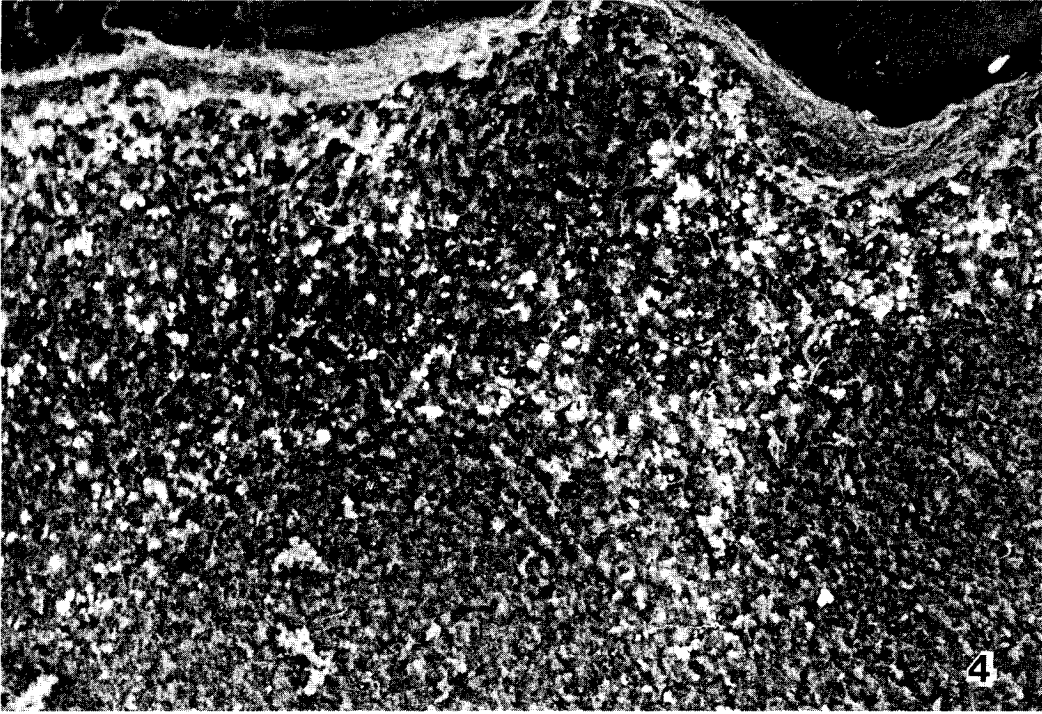


Fig. 4. Scanning electron micrograph of a regional lymph node 7 days after tungsten deposition in the airway. A high density of tungsten inclusions (white spots) is seen in the subcapsular and interfollicular sinuses of the node. $\times 1050$.

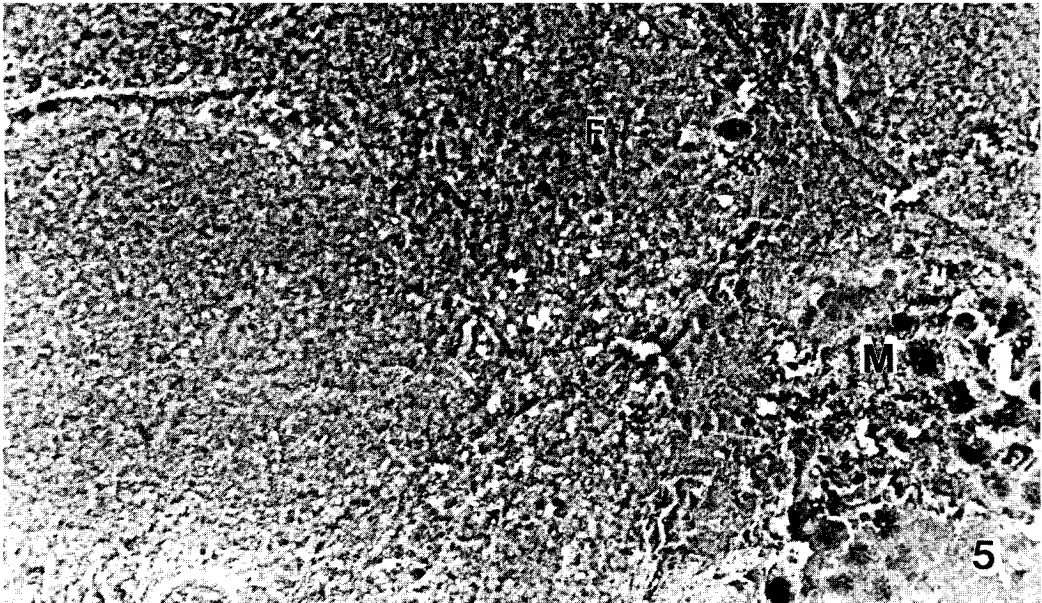


Fig. 5. Scanning electron micrograph of the cortex-medulla transition of regional lymph node 7 days after airway deposition of tungsten. The metal inclusions (white spots) are concentrated at the paracortical region. Light and small-sized tungsten deposition is observed in the follicle area (F). M = lymph node medulla. $\times 470$.

Topography of particle-laden macrophages in the lymph node

The distribution of tungsten-positive macrophages in the different anatomical domains of the regional lymph node was studied by scanning electron microscopy using elemental particle analysis to specifically identify tungsten (with this analytical mode the tungsten deposits appeared as white spots in scanning electron micrographs). The method allowed the detection of very low quantities of tungsten as exemplified by *Fig. 2A and 2B* from a lymph node virtually devoid of tungsten: here, just one single tungsten-positive cell was present in a large area of a subcapsular sinus. At day 3, the few tungsten-positive macrophages seen in the regional lymph node were located in the subcapsular area, sometimes in association with trabecular extensions of the connective tissue of the capsule that occasionally continued into the lymph node cortex (*Fig. 3*). At day 7 and 14 there was a massive accumulation of tungsten-positive cells in the subcapsular sinus; in these samples we found an even distribution of the tungsten-laden macrophages throughout this area. A high density of tungsten-bearing macrophages was also detected at day 7 in the narrow interfollicular areas of the lymph node (*Fig. 4*); a moderate number of tungsten-positive cells was observed in the medullary cords, and in the paracortical zone, in particular where the interfollicular sinuses joined with the outer medulla (*Fig. 5*). In some lymph nodes, the follicular domains contained minute amounts of tungsten that were scattered as small inclusions associated with dendritic cells (*Fig. 4*). The diagram in *Fig. 6* summarizes our results on the sequential topography of tungsten-positive cells in the lymph node.

High magnification views of tungsten-positive areas of the lymph node showed that virtually all inclusions were intracellularly located. The tungsten bodies were often segregated into a polar patch at the periphery of macrophages, rather than dispersed throughout cytoplasm (*Figs. 7A and 7B*). By thin section

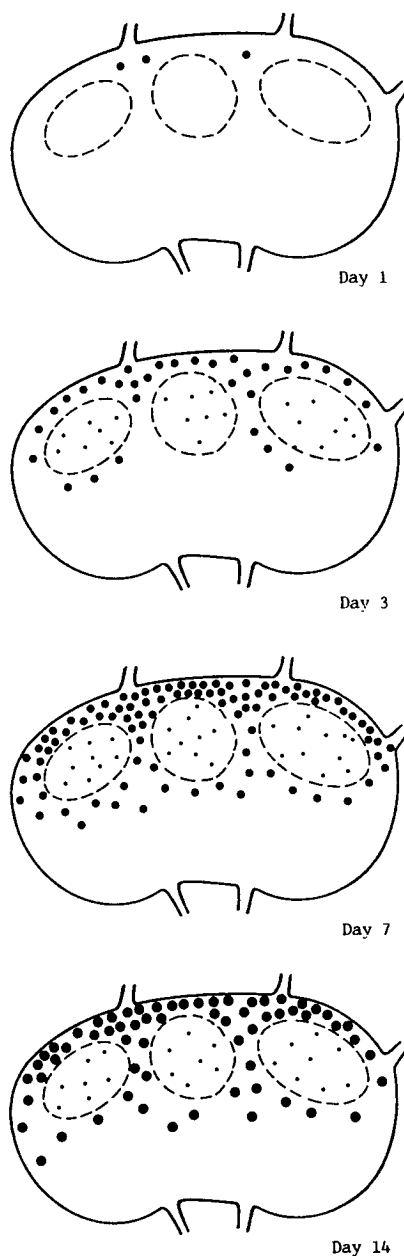


Fig. 6. Diagram that summarizes our topographical data on the sequential distribution of tungsten in the lymph node (a saggital section of a lymph node is depicted; the hilus is at the bottom of the drawing). The tungsten inclusions are represented by black dots; the distinct diameters of the dots express differences found in the size of the tungsten intracellular inclusions.

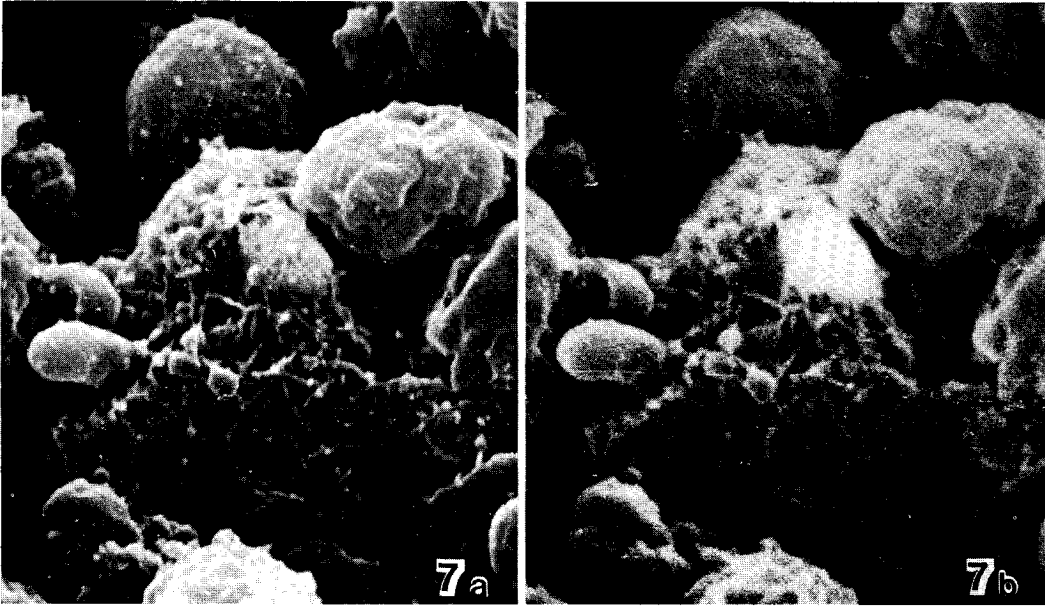


Fig. 7. High magnification scanning electron micrographs (a--routine SEM mode; b--tungsten detection by the elemental analysis mode) of interfollicular domain of regional lymph node 7 days after airway instillation of tungsten. One of the macrophages shown contains a single, large inclusion of tungsten (white spot in figure b). By comparing the two images, it can be concluded that the intracellular inclusion is located at the cell periphery. x18,000.

electron microscopy, the tungsten inclusions showed a characteristic "paracrystalline" outline (Fig. 8, arrowhead). The inclusions remained inside vesicles showing a matrix with a heterogeneous electron-dense appearance suggestive of previous fusion of lysosomes with tungsten-containing phagosomes (Figs. 8 and 9).

At day 7 and 14 numerous instances of intimate surface contact between tungsten-positive macrophages and lymphocytes were found at the lymph node medullary cords. Here, the lymphocytes associated with tungsten-positive macrophages often depicted the distinctive ultrastructural features of the plasma cell, i.e., a striking hypertrophy of the rough endoplasmic reticulum and of the Golgi apparatus. This appearance is illustrated in Fig. 9 where a tungsten-bearing macrophage and a plasma cell interact through intricate interdigitations of their plasma membranes.

DISCUSSION

After instillation of calcium tungstate (CaWO_4) particles into the airway of the left apical lobe, particle translocation to the hilar lymph nodes of the dog lung appears to be a slow process in that the percentage of tungsten-positive cells detected in the lymph node was minimal or absent at 24 hours, moderate at day 3 (6%), and reached its peak at day 7 (22%). The slow sorting of exogenous particles from lung to regional nodes is possibly due to the rarity of lymphatic vessels at the alveolar septa (15-18). The paucity of alveolar lymphatic pathways requires particle transport by macrophages through mesenchymal tissue until the first available lymphatic capillaries are reached at the respiratory bronchiole. In other words, alveolar-lymph node translocation of particles requires phagocytosis,

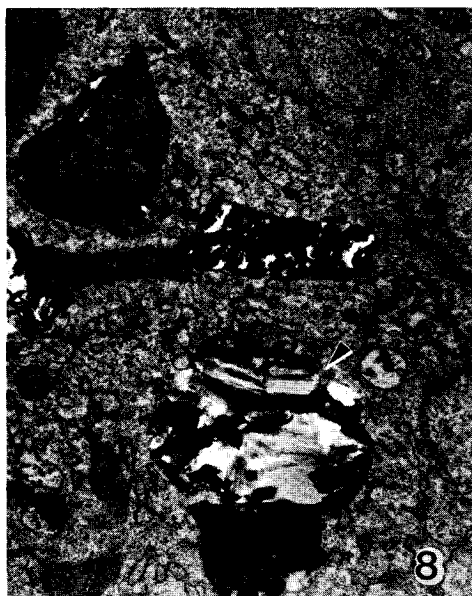


Fig. 8. Thin section micrograph of a parafollicular macrophage of the regional lymph node 7 days after tungsten instillation in the lung airway. Several tungsten-containing vesicles are observed; the metal has a "paracrystalline" appearance (arrowhead). The vesicles have a heterogeneously electron dense content that is suggestive of previous fusion with lysosomes. $\times 12,000$.

and interpretation in accordance with the results of Harmsen et al (9).

Besides tungsten-positive macrophages, we also found an increased number of granulocytes in the hilar lymph node at day 3 after CaWO_4 instillation. The relative contribution of these granulocytes to the transport of the tungsten salt is probably small since we seldom saw tungsten-positive granulocytes in the lymph node. The granulocytes reached the lymph node before the arrival of the first tungsten-positive macrophages. Phagocytosis of the granulocyte by the macrophage at inflammatory sites may enhance activation and antimicrobial capacity of the macrophage (19-21).

In addition to the regional, apical left lymph node, tungsten was also detected, at day 14, in the large medial and in the right upper node. This finding suggests the presence of contralateral lymphatic drainage pathways in the pulmo-

nary system, an arrangement that may explain the bilateral spread of infectious agents and tumor cells in the lung (22,23).

Based on the *in situ* detection of tungsten in hilar lymph nodes by scanning electron microscopy, we outlined a sequential mapping (see Fig. 6) of the lymph node domains where metal particles became sorted. Virtually all of the lymph node tungsten was inside macrophages, a finding confirmed by light microscopic analysis of Epon-embedded samples and by thin section electron microscopy. The subcapsular space was the first region of the node to receive tungsten-positive macrophages. The even distribution of macrophages in this area indicated that this site was continuous in the dog node contrary to the rat (6). The interfollicular trabecular sinuses were the pathway used by migrating macrophages to reach the medullary zone. The sinuses were narrow and conceivably slowed the sorting of subcapsular macrophages in the medulla. Moderate numbers of particle-bearing macrophages were also detected, in the paracortical domain of the node, a T-cell dependent region (3), and within the medullary cords, a B-cell differentiation region. In the latter domain (the medullary cords) there was intricate cell-to-cell interactions between tungsten-positive macrophages and plasma cells. The biological significance of this extensive interaction was difficult to assess because tungsten was a non-antigenic element. Nonetheless, the exuberance of these intercellular contacts deserve further investigation.

Some of the lymphoid follicles contained tungsten, albeit in scattered and minimal amounts. These small quantities of tungsten were associated with dendritic cells. Because penetration of lymphoid follicles by tungsten-positive macrophages was not observed it was likely that, in the lymph node, tungsten was transferred in small amounts from parafollicular macrophages to follicular dendritic cells. These findings and interpretation are in contrast with previous studies in the mouse and in the guinea pig describing a massive pene-

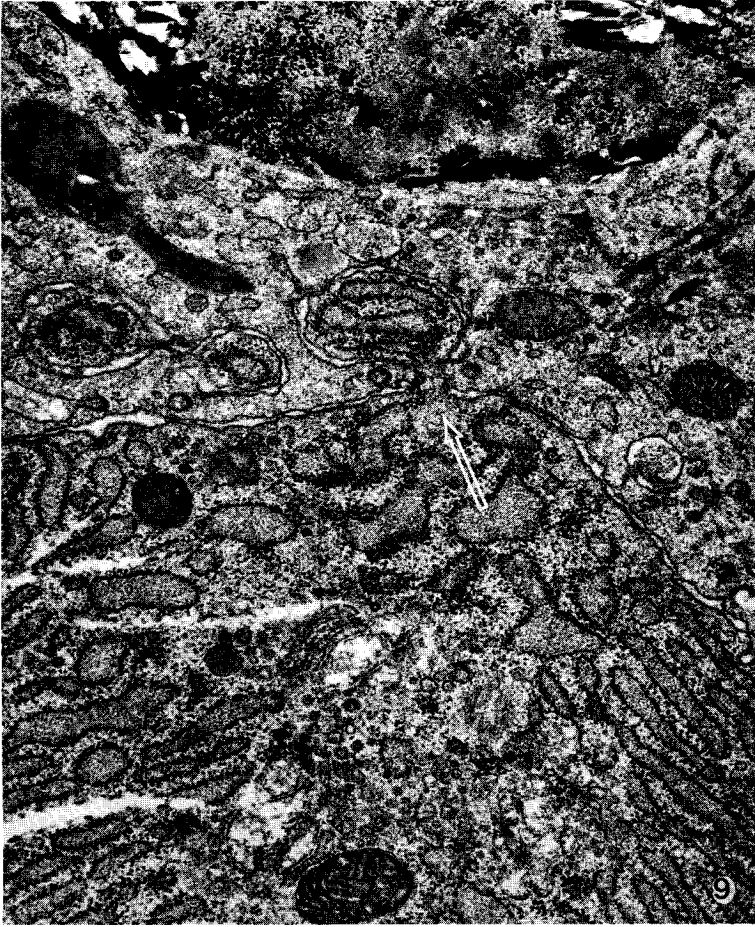


Fig. 9. Thin section electron micrograph showing intimate surface interaction between a tungsten-containing macrophage (top of the figure) and a plasma cell (bottom of the figure) at a medullary cord of the lymph node. A fingerlike extension (arrow) of the plasma cell cytoplasm is encircled by the macrophage (two other macrophage-embraced prolongations of the plasma cell are seen on the left side of the figure). Note the characteristic hypertrophy of the rough endoplasmic reticulum and of the Golgi apparatus in the plasma cell, and the presence of tungsten (dark inclusion at the top of the figure) inside the macrophage. x38,000.

tration of the germinal center by particle-carrying lymph macrophages (24,25). Instead, the data are more compatible with the view that, on reaching the follicle periphery, the inflammatory macrophages transfer particulate antigen to dendritic cells rather than carry the antigen further into the core of the follicle (26).

ACKNOWLEDGEMENTS

We are grateful to Professor Manuel Teixeira de Silva for suggestions throughout the course of this study and for critical evaluation of the manuscript. We thank Drs. Nair Esaguy, Paula Ferreira da Silva, and Rui Appelberg for

reading the text, Mr. Alfredo Ribeiro for surgical help, Mr. Anselmo Carraça and Mrs. Maria Teresa Oliveira for the drawings, and Dr. Abel Roldão and Mrs. Andrea Costa for photographic work. This investigation was supported by a research grant from the Junta Nacional de Investigação Científica e Tecnológica (Science Research Council of Portugal).

REFERENCES

1. van Rooijen, M: The "in situ" immune response in lymph nodes: A review. *Anat. Rec.* 218 (1987), 359.
2. De Sousa, MAB, DMY Parrott, EM Pantelouris: The lymphoid tissues in mice with congenital aplasia of the thymus. *Clin. Exp. Immunol.* 4 (1969), 637.
3. Parrott, DMY, MAB De Sousa: Thymus-dependent and thymus-independent populations: Origin, migratory patterns and lifespan. *Clin. Exp. Immunol.* 8 (1971), 663.
4. Parrott, DMY, MAB De Sousa, J East: Thymus-dependent areas in the lymphoid organs of neonatally thymectomized mice. *J. Exp. Med.* 123 (1966), 191.
5. Brownstein, DG, AH Rebar, DE Bice, et al: Immunology of the lower respiratory tract. Serial morphologic changes in the lungs and tracheobronchial lymph nodes of dogs after intrapulmonary immunization with sheep erythrocytes. *Am. J. Pathol.* 98 (1980), 499.
6. Sante-Marie, G, F-S Peng, C Bélisle: Overall architecture and pattern of lymph flow in the rat lymph node. *Am. J. Anat.* 164 (1982), 275.
7. Heath, TJ, HJ Spalding: Pathways of lymph flow to and from the medulla of lymph nodes in sheep. *J. Anat.* 155 (1987), 177.
8. Szakal, AK, MH Kosco, JG Tew: Microanatomy of lymphoid tissue during humoral immune responses: Structure function relationships. *Ann. Rev. Immunol.* 7 (1989), 91.
9. Harmsen, AG, BA Muggenberg, MP Snipes, et al: The role of macrophages in particle translocation from lungs to lymph nodes. *Science* 230 (1985), 1277.
10. Harmsen, AG, MJ Mason, BA Muggenberg, et al: Migration of neutrophils from lung to tracheobronchial lymph node. *J. Leukocyte Biol.* 41 (1987), 95.
11. Bice, DE, DL Harris, JO Hill, et al: Local and systemic immunity following localized deposition of antigen in the lung. *Chest* 75S (1979), 246S.
12. Haley, PJ, DE Bice: Immune reactions in the pulmonary system. In *Toxicology of the Lung*, Gardner, DE, JD Crapo, EJ Massaro (Eds.), Raven Press, New York (1988), 407.
13. Silva, MT: The use of transmission electron microscopy of ultrathin sections for the characterization of normal and damaged bacterial membranes. In *Biomembranes: Dynamics and Biology*, Guerra, FC, RM Burton (Eds.), Plenum Press, New York (1984), 1.
14. Silva, MT: Uranyl salts. In *Encyclopedia of Microscopy and Microtechnique*, Gray, P (Ed.), Van Nostrand Reinhold Co., New York (1973), 585.
15. Grande, NR: *Pulmonary Arterial Hypertension*. Ph.D. Thesis. University of Porto, Portugal (1965).
16. Grande, NR, J Ribeiro, M Soares, et al: The lymphatic vessels of the lung: Morphological study. *Acta Anat.* 115 (1983), 302.
17. Grande, NR, O Yeep, E Carvalho, et al: Alveolar septal changes in pulmonary edema: A subcellular study of lung clearance in the dog. *J. Submicrosc. Cytol.* 19 (1987), 43.
18. Leak, LV, MP Jamuar: Ultrastructure of pulmonary lymphatic vessels. *Am. Rev. Respir. Dis.* 128 (1983), S59.
19. Chapes, SK, S Haskill: Evidence of granulocyte-mediated macrophage activation after *C. parvum* immunization. *Cell. Immunol.* 75 (1983), 367.
20. Heifets, L, K Imai, MB Goren: Expression of peroxidase-dependent iodination by macrophages ingesting neutrophil debris. *J. Reticuloendoth. Soc.* 28 (1980), 391.
21. Silva, MT, MNT Silva, R Appelberg: Neutrophil-macrophage cooperation in the host defence against mycobacterial infections. *Microbiol. Pathogenesis* 6 (1989), 369.
22. Martini, N, BJ Flehinger, MB Zaman, et al: Results of resection in non-oat cell carcinoma of the lung with mediastinal lymph node metastases. *Ann. Surg.* 198 (1983), 386.
23. Libshitz, HI, RJ McKenna, CF Moun-tain: Patterns of mediastinal metastases in bronchogenic carcinoma. *Chest* 90 (1986), 229.

24. Kotani, M, K Okada, H Fujii, et al: Lymph macrophages enter the germinal center of lymph nodes of guinea pigs. *Acta Anat.* 99 (1977), 391.
25. Kotani, M, T Ezaki, H Fujii, et al: Peritoneal macrophages introduced into mouse foot pads enter the germinal center of regional lymph nodes non-specifically. *Acta Anat.* 104 (1979), 406.
26. Heinen, E, N Cormann, C Kinet-Denoel: The lymph follicle: A hard nut to crack. *Immunol. Today* 9 (1988), 240.

Nuno Rodrigues Grande, M.D., Ph.D.
Professor and Chairman
Department of Anatomy
Abel Salazar Institute for the
Biomedical Sciences
Largo Prof. Abel Salazar
4000 Porto PORTUGAL